Influence of Anterior Mitral Leaflet Second-Order Chordae Tendineae on Left Ventricular Systolic Function

Sten Lyager Nielsen, MD, PhD; Tomasz A. Timek, MD; G. Randall Green, MD; Paul Dagum, MD, PhD; George T. Daughters, MS; J. Michael Hasenkam, MD; Ann F. Bolger, MD; Neil B. Ingels, PhD; D. Craig Miller, MD

Background—The contribution of anterior mitral leaflet second-order ("strut") chordae tendineae to left ventricular (LV) systolic mechanics is debated; we measured the in vivo contribution of anterior chordae tendineae (ACT) and posterior chordae tendineae (PCT) to regional and global LV contractile function.

Methods and Results—Eight sheep had radiopaque markers implanted in the LV epicardium, partitioning the ventricle into 12 regions. Microminiature force transducers and snares were sutured to anterior leaflet "strut" chordae originating from ACT and PCT papillary muscles. Chordal tension, marker images, and hemodynamic data were acquired before and after (CUT) severing ACT and PCT. Fractional area shrinkage and slope of the regional end-diastolic area–regional stroke work relation (r-PRSW) were computed for each LV region. CUT did not affect global LV systolic function but reduced FAS in LV segments near the PCT insertion site: equatorial posterior lateral (19±2% versus 16±2%, $P<0.05$), apical posterior lateral (23±4% versus 19±4%, $P<0.05$), and posterior medial LV segments (16±2% versus 13±2%, $P<0.05$). r-PRSW fell near both the ACT (equatorial anterior medial [84±8 versus 62±11 mm Hg, $P<0.05$] and lateral [73±7 versus 53±9 mm Hg, $P<0.05$]) and PCT (apical posterior medial [91±12 versus 67±17 mm Hg, $P<0.05$] and lateral [72±8 versus 59±9 mm Hg, $P<0.05$]) LV insertion sites. Maximum tension in PCT was higher than in ACT (0.81±0.1 versus 0.52±0.08*N*, $P<0.01$).

Conclusions—Dividing anterior leaflet strut chordae in sheep was associated acutely with regional LV systolic dysfunction near the chordal insertion sites. Caution is necessary when embarking on procedures that cut second-order chordae to treat ischemic mitral regurgitation, since this may compromise LV systolic function in ventricles that are already impaired. **(*Circulation*. 2003;108:486-491.)**

Key Words: mechanics ■ regurgitation ■ ventricles ■ mitral valve

Since Lillehei et al[1] introduced the concept of mitral valve–left ventricular (LV) interaction, clinical[2,3] and experimental[4] studies demonstrated that preserving the chordae tendineae during mitral valve surgery improves postoperative LV systolic function and clinical outcome. The chordae tendineae are commonly classified according to their insertion sites on the mitral leaflets.[5] The first-order (primary or "marginal") chordae insert on the leaflet free edges, the second-order (or "strut") chordae insert on the ventricular surface of the leaflets, usually near the junction between the rough and smooth zones, and the third-order chordae arise directly from the LV wall. The anterior mitral valve leaflet (AMVL) second-order chordae also have different origins within the ventricle. The anterolateral second-order chordae and papillary muscle originate in the midportion of the anterior LV wall, whereas the posteromedial second-order chordae and papillary muscle originate in the apical-posterior LV region. Second-order chordal transposition can be used to correct anterior mitral valve leaflet prolapse[6,7]; cutting second-order chordae recently has been recommended as a surgical treatment for ischemic mitral regurgitation (IMR) to alleviate leaflet apical tethering during systole.[8] The in vivo effects of sacrificing second-order chordae on regional LV systolic function, however, have not been investigated. Since the mitral subvalvular apparatus has the dual role of preventing mitral leaflet prolapse as well as optimizing LV systolic pump function, knowing the functional role of the chordae tendineae should provide a more rational basis for mitral repair procedures that alter normal chordal anatomy. One study indicated that the second-order chordae are involved

Received October 24, 2002; revision received April 10, 2003; accepted April 14, 2003.

From the Department of Cardiothoracic and Vascular Surgery and Institute of Experimental Clinical Research, Aarhus University Hospital, Skejby Sygehus, Aarhus, Denmark (S.L.N., J.M.H.); the Department of Cardiothoracic Surgery, Stanford University School of Medicine, Stanford, Calif (T.A.T., G.R.G., P.D., G.T.D., N.B.I., D.C.M.); the Division of Cardiology, University of California San Francisco (A.F.B.); and the Laboratory of Cardiovascular Physiology and Biophysics, Research Institute, Palo Alto Medical Foundation, Palo Alto, Calif (G.T.D., N.B.I.).

Presented in part at the 72nd American Heart Association Annual Scientific Sessions, Atlanta, Ga, November 1999.

Correspondence to D. Craig Miller, MD, Department of Cardiothoracic Surgery, Falk Cardiovascular Research Center, Stanford University School of Medicine, Stanford, CA 94305-5247. E-mail dcm@stanford.edu

Circulation **is available at http://www.circulationaha.org** **DOI: 10.1161/01.CIR.0000080504.70265.05**

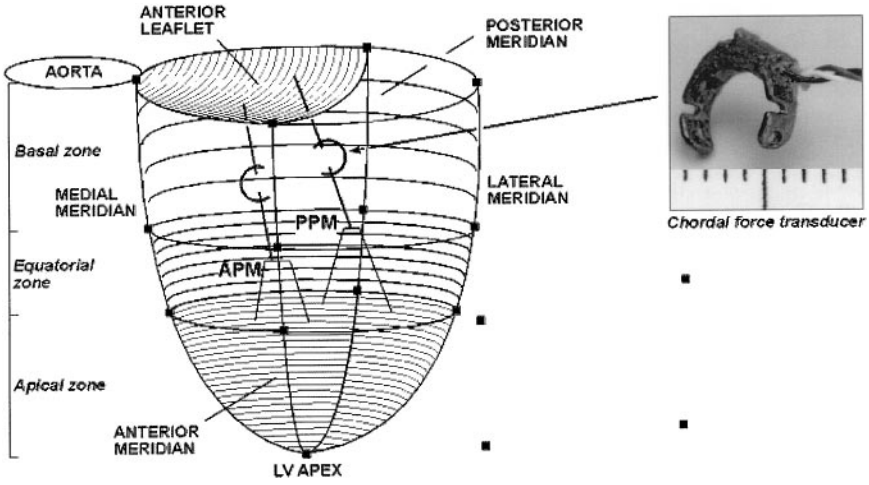

Figure 1. Myocardial marker array used in the experiment. Each regional area defined by 4 markers was calculated as the sum of two triangular planar areas ($rArea_1$ and $rArea_2$). Chordal force transducers were attached to the two AMVL strut chordae tendineae. APM indicates anterior papillary muscle; PPM, posterior papillary muscle.

predominantly in valvular-ventricular interaction, whereas first-order AMVL chordae prevent leaflet prolapse and mitral regurgitation (MR).[9] That experiment, however, was performed in an isolated working pig heart model that used load-dependent measures to assess LV systolic function. No investigation of the in vivo influence of second-order chordae on LV systolic function exists. Furthermore, the distribution of tension between anterior and posterior AMVL chordae has not been studied in an intact animal preparation, yet such data coupled with regional indexes of LV function would further elucidate the complex relation of valvular-ventricular interactions.

Hypothesizing that severing second-order chordae tendineae would adversely perturb regional LV systolic function, we implanted radiopaque myocardial markers and force transducers in sheep to measure regional and global LV systolic function and AMVL strut chordae tension before and after cutting both AMVL strut chordae.

Methods

Surgical Preparation

Eight adult male sheep were used. Details about the chordal miniature force transducer[10] and radiopaque marker[11,12] implantation techniques have been described previously. Eight tantalum helixes were inserted into the subepicardial LV layer along 4 equally spaced LV longitudinal meridians at 2 levels between LV apex and base (Figure 1), with one at the LV apex. After establishment of cardiopulmonary bypass and cardioplegic arrest, 4 miniature markers were sutured equidistantly (approximately every 90°) around the circumference of the mitral annulus. These 13 markers divided the LV epicardium surface into 12 regions: Four at the LV base, 4 equatorial, and 4 (triangular) regions near the LV apex. Based on previous investigations of mitral subvalvular geometry in sheep[13] and dogs,[14] we knew that the anterolateral second-order chordae and papillary muscle insert in the anterior wall of the LV equatorial zone, whereas the posteromedial second-order chordae and papillary muscle insert in the posterior region of the apical-equatorial zone. The largest of the second-order chordae inserting on the AMVL and emanating from each papillary muscle, commonly referred to as "strut" chordae (anterior chordae tendineae [ACT] and posterior chordae tendineae [PCT], originating from the anterior and posterior papillary muscles, respectively) were identified, and miniature chordal force transducers were sutured to these chordae with chordal continuity maintained in series with the implanted transducers.[10] Wire snares were secured around these chordae below the force transducer and exteriorized through the LV wall. A micromanometer pressure transducer (PA4.5-X6; Konigsberg Instruments, Inc) was placed in the LV chamber through the apex, and pneumatic occluders were placed around the superior and inferior vena cava. The animals were weaned from cardiopulmonary bypass, transferred to the experimental catheterization laboratory, and studied intubated with the chest open, with the use of continuous ketamine (1 to 4 mg/kg per hour IV infusion) and diazepam (5 mg IV bolus as needed) anesthesia. Simultaneous biplane videofluoroscopy (60 Hz) and hemodynamic data were recorded over a range of LV filling volumes (preload reduction using vena caval occlusion). Data were acquired sequentially after random transection of one set of chordae and then the other by passing electrocautery radiofrequency current through the externalized wire snares; the small numbers (PCT was cut first in 5 animals, ACT first in 3 animals) precluded statistical comparison of the effect of isolated ACT versus PCT division on regional LV systolic function. Therefore, only 2 experimental conditions were studied: (1) baseline (control), and (2) after cutting both second-order AMVL chordae (CUT). Epicardial color Doppler echocardiography confirmed chordal transection and graded MR on a 0 to +4 scale (none, mild, moderate, moderate-severe, severe). All animals received humane care, in compliance with the "Principles of Laboratory Animal Care" formulated by the National Society for Medical Research and the "Guide for Care and Use of Laboratory Animals" prepared by the National Academy of Sciences and published by the National Institutes of Health (DHEW NIHG Publication 85–23, revised 1985). This study was approved by the Stanford Medical Center Laboratory Research Animal Review committee and conducted according to Stanford University policy.

Data Acquisition

Images were acquired with the animal in the right lateral position, using a Philips Optimus 2000 biplane Lateral ARC 2/Poly DIAGNOST C2 system (Phillips Medical Systems, North America Company), with the image intensifiers in the 9-inch mode. Data from two radiographic views were digitized and merged to yield 3-dimensional coordinates for each of the radiopaque markers every 16.7 seconds, using custom-designed software.[15,16] The chordal force transducers were coupled in a Wheatstone half-bridge to a strain-gauge amplifier (Model 2021, Measurement Group Inc). During data acquisition chordal force, LV pressure, and ECG voltage analog signals were simultaneously digitized and recorded.

Data Analysis

Hemodynamic and Cardiac Cycle Timing Markers

Three consecutive steady-state beats before and after cutting both second-order AMVL chordae were averaged and defined as the "control" and "CUT" data for each animal, respectively. End systole was defined as the videofluoroscopic frame after peak rate of LV pressure fall ($-dP/dt_{max}$), whereas end diastole was defined as the

frame containing the peak of the ECG R wave. Instantaneous LV volume was calculated every 16.7 ms from epicardial markers through the use of a space-filling multiple tetrahedral volume method. Since LV wall mass is included in this calculation of LV volume, this method overestimates actual LV chamber volume but accurately reflects relative changes in LV chamber size.[17]

Indexes of Regional LV Systolic Function

Left ventricular fractional area shrinkage (FAS) and regional preload-recruitable stroke work (r-PRSW) were used as indexes of regional LV systolic function; both have been validated in sheep models.[12] Each LV region defined by 4 markers was divided into 2 triangular planar areas (Figure 1); the regional area was then computed as the sum of the areas of the triangles. The fractional change in epicardial area was calculated as $FAS=100\% \cdot ([rArea_{MAX}-rArea_{MIN}]/rArea_{MAX})$, where $rArea_{MAX}$ was the maximum regional area and $rArea_{MIN}$ was the minimum regional area during the cardiac cycle. Paralleling assessment of global LV pressure-volume relations, the LV pressure-regional LV epicardial area relation of each of the 12 epicardial regions was computed before and after chordal transection at steady state and during abrupt preload reduction. Regional LV stroke work was calculated as the integral (from maximum to minimum regional epicardial area) of LV pressure multiplied by regional epicardial area (A_r) for each cardiac cycle at baseline and during caval occlusion: $rSW=\int LV\ pressure \cdot dA_r$.

A regional preload-recruitable stroke work surrogate (r-PRSW) was then obtained by linear regression of rSW against regional area at end diastole (EDA_r): $rSW=rM_w \cdot (EDA_r-rA_w)$, where rM_w and rA_w are the slope and area axis intercept, respectively. Although this measure has units of force, it is similar to the "linearized Frank-Starling relation" described by Glower et al.[18] We have previously shown that the slope (rM_W) of the r-PRSW versus maximum area relation consistently reflects changes in LV inotropic state in all LV epicardial regions.[12] Global PRSW was calculated from the stroke work–end-diastolic volume relation during preload occlusion, and end-systolic elastance (E_{es}) was determined from end-systolic volume–LV pressure curves in each animal.

Inspection of raw data revealed that heterogeneous reductions in LV regional area and LV pressure during caval occlusion occasionally resulted in negative rSW or in a discontinuous fall in end-diastolic area–rSW data points, and linear regression of these data sets to calculate rM_W showed low correlation coefficients. Among 192 individual load-insensitive measurements of r-PRSW, all data from 1 animal and 8 individual data points from 6 other animals were excluded from the analysis to avoid these erroneous values, that is, negative slopes.

Statistical Analysis

All data are reported as mean±1 SEM, unless otherwise stated. Hemodynamic, chordal force, and marker-derived data from 3 consecutive steady-state beats in each heart were aligned at end diastole (t=0) and averaged for control and CUT conditions. Peak chordal force during systole in the two strut chordae was compared by means of the 2-tailed *t* test for paired comparisons. Comparisons of FAS and slope (rM_W) of r-PRSW were made by using repeated-measures ANOVA, with the LV epicardial region representing the nonrepeated factor and CUT representing the repeated factor. Changes with CUT detected by a significant *F* value were analyzed further by using the Student's *t* test for paired observations to identify which individual regions changed significantly.

TABLE 1. Hemodynamics

	Control	CUT
HR, bpm	107±4	107±4
LV pressure, mm Hg	101±3	89±7
LV +dP/dt, mm Hg per s	2484±145	2160±277
LV EDV, mL	200±21	192±22
LV EDP, mm Hg	12±1	12±2
E_{es}, mm Hg/mL	2.3±0.4	1.9±0.5
PRSW, mm Hg	62±4	54±7

HR indicates heart rate; +dP/dt, peak positive rate change of LV pressure; LV, left ventricular; EDV, end-diastolic volume; EDP, end-diastolic pressure; E_{es}, global LV end-systolic elastance; PRSW, global LV preload-recruitable stroke work.

Data expressed as mean±1 SEM.

Results

Animal weight averaged 72±4 kg; cardiopulmonary bypass time was 202±9 minutes, with a cross-clamp time of 132±5 minutes. Postmortem examination revealed the markers to be in proper position and confirmed complete transection of the two thicker strut chordae. There was no difference in hemodynamic parameters before and after severing the second-order chordae (Table 1). Both load-dependent and load-independent indexes of global LV systolic function did not change with cutting the strut chordae. Trace to mild MR was detected in all Control group animals, and there was no change in the degree of MR after cutting both second-order chordae (0.8±0.2 [control] versus 0.6±0.2 [CUT]; *P*=NS).

Chordal Tension

The mean tension in the anterolateral (ACT) and posteromedial (PCT) strut chordae throughout the cardiac cycle is illustrated in Figure 2 (left panel). The maximum tension in the PCT was higher than that in the ACT during systole (0.81±0.1*N* versus 0.52±0.08*N*, respectively; *P*<0.01). Figure 1 (right panel) illustrates the group mean relation between

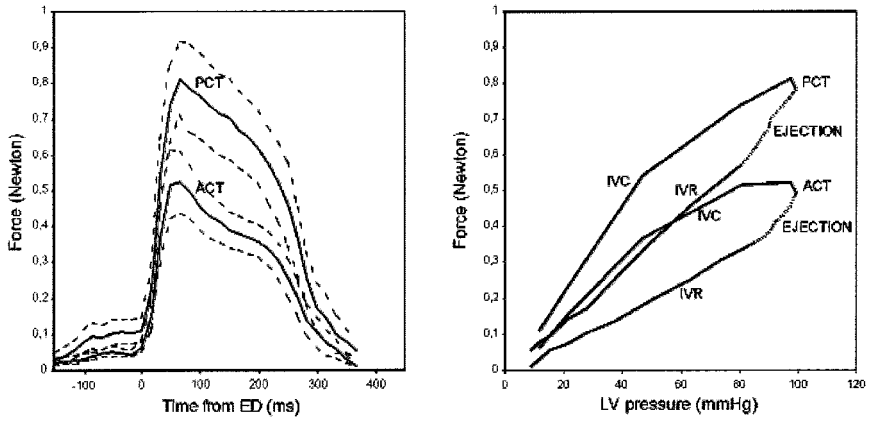

Figure 2. Left, Group mean data for systolic tension of the AMVL anterolateral (ACT) and posteromedial (PCT) strut chordae tendineae during control. Dashed lines indicate ±1 SEM; ED, end diastole (t=0). Right, Group mean data for tension of ACT and PCT with respect to LV pressure during systole. Note bilinear relation between LV pressure and chordal tension during isovolumic contraction (IVC), a decrease in chordal tension despite high LV pressure during ejection, and an almost linear decline during isovolumic relaxation (IVR).

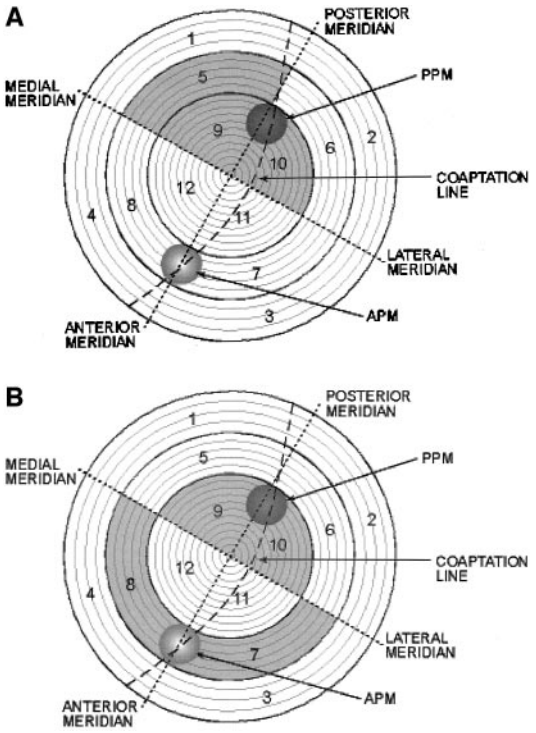

Figure 3. Schematic of the LV wall regions (1 to 12) as viewed from the mitral annulus (perimeter) toward the LV apex (center). A, Striped areas indicate LV regions where FAS fell significantly after chordal transection (see Table 2). B, Striped areas indicate LV regions where the slope (rM_W) of regional preload-recruitable stroke work fell significantly after chordal transection (see Table 3). Chordal insertion sites of the anterior (APM) and posterior papillary muscle (PPM) into the LV wall are shown. Curved dashed line indicates mitral leaflet coaptation line.

LV pressure and chordal tension throughout systole. It represents a bilinear, direct relation during isovolumic contraction, a decrease in chordal tension during ejection despite high LV pressure, and a linear fall in tension during isovolumic relaxation.

Regional LV Systolic Function

FAS in all LV epicardial regions before and after severing the strut chordae is summarized in Table 2. After chordal transection, FAS decreased in the apical and equatorial regions along the posterior meridian (regions 5, 9, and 10) adjacent to the PCT insertion site (Figure 3A). Although FAS is a load-dependent measure of regional LV contractility and could have been affected by changes in regional EDV, the observed reductions in FAS were consistent with load-independent measurements of regional LV systolic function. After CUT, the slope (rM_W) of regional preload-recruitable stroke work (a load-independent measure of regional LV systolic function) decreased in the anteroequatorial regions (regions 7 and 8) adjacent to the ACT insertion site and in the apical regions near the PCT insertion site (regions 9 and10) (Figure 3B).

TABLE 2. LV Regional Fractional Area Shrinkage

		FAS (%)			
		Control		CUT	
Region		Mean±SEM	(Min-Max)	Mean±SEM	(Min-Max)
Basal					
1	PM	17±3	(9–30)	17±3	(7–30)
2	PL	20±3	(12–31)	18±3	(8–33)
3	AL	20±3	(13–25)	17±2	(7–24)
4	AM	14±1	(7–20)	13±1	(10–15)
Equatorial					
5	PM	19±2	(11–26)	16±2*	(8–25)
6	PL	18±2	(13–26)	15±2	(9–24)
7	AL	21±1	(16–25)	18±2	(8–25)
8	AM	21±2	(14–29)	18±1	(12–25)
Apical					
9	PM	16±2	(10–23)	13±2*	(8–21)
10	PL	23±4	(13–48)	19±4*	(10–42)
11	AL	18±1	(11–22)	15±2	(8–19)
12	AM	18±2	(12–28)	16±2	(9–24)

FAS indicates fractional area shrinkage; AL, anterolateral; AM, anteromedial; PL, posterolateral; PM, posteromedial. Data expressed as mean±1 SEM (min–max). *$P<0.05$ vs control; Student's t test used for paired observations.

Discussion

Although transposition[6] or even "therapeutic" cutting[8] of the anterior leaflet strut chordae is used clinically, the physiological function of the AMVL second-order chordae is unknown. The present experiment revealed that tension in the AMVL strut chordae increased rapidly during LV pressure rise in early systole, and maximum chordal tension coincided with maximum LV pressure. Tension in the AMVL strut chordae during systole, however, was not due solely to LV pressure; the nonlinear relation could not be accounted for by changes in mitral leaflet shape or chordal insertion geometry. Valve competence, leaflet edge separation, and leaflet geometry were not altered by cutting the second-order AMVL chordae,[19] even though the forces in the chordae are transmitted to the LV myocardium. Dividing the AMVL strut chordae caused regional LV systolic dysfunction in the regions adjacent to the ACT and PCT insertion sites: r-PRSW was reduced near both chordal insertion sites, and FAS was lower in the LV regions subtending the PCT insertion site. This distinction is important because FAS is a load-dependent measure of muscle performance, whereas r-PRSW is a load-independent measure of contractile function.

Baseline tension in the PCT was higher than the tension of the ACT. Because the ACT and the anterior papillary muscle insert on the (less curved) LV free wall and theoretically in a region of higher wall stress, we had expected the opposite finding. One interpretation is that the PCT are more important than ACT in terms of LV systolic contractile function; however, this experiment was not designed to evaluate the isolated effects of ACT versus PCT division. It is noteworthy that both FAS and r-PRSW were reduced in the LV regions near the PCT insertion, whereas only r-PRSW decreased in the regions of ACT insertion after chordal transection. Whether this is related to the differential load distribution of the chordae remains speculative. Severing both strut chordae

TABLE 3. LV Regional Preload-Recruitable Stroke Work

		r-M_W (mm Hg)			
		Control		CUT	
Region		Mean±SEM	(Min–Max)	Mean±SEM	(Min–Max)
Basal					
1	PM	70±25	(19–241)	63±16	(13–151)
2	PL	48±10	(26–103)	41±11	(7–76)
3	AL	56±12	(24–132)	67±19	(9–157)
4	AM	42 ±4	(1–59)	42 ±9	(6–73)
Equatorial					
5	PM	84±11	(54–145)	80±17	(14–161)
6	PL	63 ±4	(51–84)	61±13	(10–124)
7	AL	73 ±7	(44–92)	53 ±9*	(13–88)
8	AM	84 ±8	(47–120)	62±11*	(7–110)
Apical					
9	PM	91±12	(48–132)	67±17*	(4–132)
10	PL	72 ±8	(50–110)	59 ±9*	(15–96)
11	AL	61±11	(32–105)	66±11	(12–117)
12	AM	80 ±9	(43–122)	76±13	(22–131)

r-M_W indicates slope of regional preload-recruitable stroke work relation; AL, anterolateral; AM, anteromedial; PL, posterolateral; PM, posteromedial.

Data expressed as mean±1 SEM (min–max).

*$P<0.05$ vs control; Student's t test used for paired observations.

had no statistically significant effect on either load-dependent or load-independent measures of global LV systolic function, but this could be due to a β (or type II) statistical error.[25]

The functional roles of the first-order and second-order chordae tendineae are difficult to isolate and define quantitatively, but in vitro as well as ex vivo observations are consistent with our experimental in vivo findings. The AMVL second-order strut chordae typically are thicker or "more stout" than the others, albeit they are more prominent in human subjects and pigs than in sheep. Collagen bundles radiate from the AMVL second-order chordal insertion sites to the trigones of the mitral annulus.[5] In a porcine study, van Rijk-Zwikker et al[20] described that the AMVL strut chordae remained taut during the cardiac cycle. From a functional viewpoint, these chordae serve as tendon-like connections between the cardiac endoskeleton and the LV free walls. Two of the coauthors recently demonstrated in an open chest preparation that the force in the strut chordae was 3-fold higher than that in the first-order chordae (0.7N versus 0.2N) in pigs.[21] Clark[22] and Kunzelman and Cochran[23] confirmed different biomechanical properties of isolated in vitro porcine first-order and second-order chordae tendineae; for the same extent of deformation, the stress in the first-order chordae was higher than that in the second-order chordae. This suggested that the stiffer first-order chordae buttress leaflet motion at valve closure to prevent leaflet prolapse, whereas the more elastic second-order chordae provide a well-balanced coupling of the LV chamber wall and the anterior leaflet. Obadia and coworkers[9] in an isolated working pig heart model showed that severing the first-order chordae resulted in leaflet prolapse and regurgitation, but fractional shortening of the mid-anterolateral LV wall (assessed by sonomicrometry) did not change. Conversely, severing the second-order chordae did not distort leaflet coaptation geometry nor cause MR but did impair anterior wall regional LV shortening.

Caution is needed when extrapolating the results of open chest animal experiments to humans; nonetheless, these observations suggest that the AMVL strut chordae enhance LV wall systolic function and are a component of valvular-ventricular interaction, corroborating the theory of differential function of the first- and second-order AMVL chordae.[9] Better understanding of the functional roles between the different types of chordae is essential to refine mitral reparative techniques. This investigation represents a step toward this goal that ultimately may require "functional mapping" of the entire mitral subvalvular apparatus (internal architecture of the ventricle). These data also serve as a warning that cutting second-order chordae to treat IMR may prove to be clinically deleterious.

Study Limitations

Many limitations exist. These data were obtained in an acute, open chest setting immediately after a long and complicated surgical procedure. Only some, not all, branches of the weblike chordal structures were divided. Only acute changes were measured; it is plausible that severing the strut chordae could result in redistribution of chordal stresses that ultimately could perturb normal LV geometry, cause mitral regurgitation, or both. Implanting the force transducers in the second-order chordae may have altered normal chordal geometry or tension. Assessment of regional LV contractile status was based on calculations of regional LV epicardial surface areas, which approximates the dynamic behavior of only the epicardial myocardial layers and does not reflect transmural dynamics throughout the LV wall. This experiment was performed in normal animal hearts. Differences in comparative anatomy between human and sheep mitral valve and subvalvular apparatus must also be considered[24]; however, because the strut chordae are thinner in ovine hearts, we would anticipate that the role of the strut chordae would be more pronounced in humans than it is in pigs.[24]

Acknowledgments

This study was supported by grants HL-29589 and HL-67025 from the National Heart, Lung, and Blood Institute; Dr Nielsen was supported by grants 97–2-3–28–22547 and 98–1-3–28–22599 from the Danish Heart Foundation. Dr Hasenkam was supported by grants 9602421 and 9602422 from the Danish National Health Research Council. Drs Green, Dagum, and Timek are Carl and Leah McConnell Cardiovascular Surgical Research Fellows and are also supported by NHLBI Individual Research Fellowship Service Awards HL-09569, HL-10000, and HL-10452, respectively. Dr Timek is a recipient of the Thoracic Surgery Foundation Research Fellowship Award. We appreciate the superb technical assistance provided by Mary K. Zasio, BA, Carol W. Mead, and Erin K. Schultz, BS.

References

1. Lillehei CW, Levy MJ, Bonnabeau RC Jr. Mitral valve replacement with preservation of papillary muscles and chordae tendineae. *J Thorac Cardiovasc Surg*. 1964;47:532–543.
2. David TE, Burns RJ, Bacchus CM, et al. Mitral valve replacement for mitral regurgitation with and without preservation of chordae tendineae. *J Thorac Cardiovasc Surg*. 1984;88:718–725.

3. Yun KL, Sintek CF, Miller DC, et al. Randomized trial of partial versus complete chordal preservation methods of mitral valve replacement: a preliminary report. *Circulation*. 1999;100(suppl II):II-90-II-94.
4. Hansen DE, Cahill PD, DeCampli WM, et al. Valvular-ventricular interaction: importance of the mitral apparatus in canine left ventricular systolic performance. *Circulation*. 1986;73:1310–1320.
5. Lam HC, Ranganathan N, Wigle ED, et al. Morphology of the human mitral valve, I: chordae tendineae: a new classification. *Circulation*. 1970;41:449–458.
6. Sousa UM, Grare P, Jebara V, et al. Transposition of chordae in mitral valve repair: mid-term results. *Circulation*. 1993;88(suppl II):II-35-II-38.
7. Grossi EA, Galloway AC, LeBoutillier M III, et al. Anterior leaflet procedures during mitral valve repair do not adversely influence long-term outcome. *J Am Coll Cardiol*. 1995;25:134–136.
8. Messas E, Guerrero JL, Handschumacher MD, et al. Chordal cutting: a new therapeutic approach for ischemic mitral regurgitation. *Circulation*. 2001;104:1958–1963.
9. Obadia JF, Casali C, Chassignolle JF, et al. Mitral subvalvular apparatus: different functions of primary and secondary chordae. *Circulation*. 1997; 96:3124–3128.
10. Nielsen SL, Nygaard H, Fontaine AA, et al. Chordal force distribution determines systolic mitral leaflet configuration and severity of functional mitral regurgitation. *J Am Coll Cardiol*. 1999;33:843–853.
11. Glasson JR, Komeda M, Daughters GT, et al. Most ovine mitral annular three-dimensional size reduction occurs before ventricular systole and is abolished with ventricular pacing. *Circulation*. 1997;96(suppl II):II-115-II-122.
12. Green GR, Dagum P, Glasson JR, et al. Semirigid or flexible mitral annuloplasty rings do not affect global or basal regional left ventricular systolic function. *Circulation*. 1998;98(suppl II):II-128-II-135.
13. Dagum P, Timek TA, Green GR, et al. Coordinate-free analysis of mitral valve dynamics in normal and ischemic hearts. *Circulation*. 2000; 102(suppl III):III-62-III-69.
14. Komeda M, Glasson JR, Bolger AF, et al. Three-dimensional dynamic geometry of the normal canine mitral annulus and papillary muscles. *Circulation*. 1996;94(suppl II):II-159-II-163.
15. Daughters GT III, Sanders WJ, Miller DC, et al. A comparison of two analytical systems for 3-D reconstruction for biplane videoradiograms. *Comp Cardiol*. 1988;15:79–82.
16. Niczyporuk MA, Miller DC. Automatic tracking and digitization of multiple radiopaque myocardial markers. *Comput Biomed Res*. 1991;24: 129–142.
17. Moon MR, DeAnda A Jr, Daughters GT, et al. Experimental evaluation of different chordal preservation methods during mitral valve replacement. *Ann Thorac Surg*. 1994;58:931–943.
18. Glower DD, Spratt JA, Snow ND, et al. Linearity of the Frank-Starling relationship in the intact heart: the concept of preload recruitable stroke work. *Circulation*. 1985;71:994–1009.
19. Timek TA, Nielsen SL, Green GR, et al. Influence of anterior mitral leaflet second-order chordae on leaflet dynamics and valve competence. *Ann Thorac Surg*. 2001;72:535–540.
20. van Rijk-Zwikker GL, Delemarre BJ, Huysmans HA. Mitral valve anatomy and morphology: relevance to mitral valve replacement and valve reconstruction. *J Card Surg*. 1994;9:255–261.
21. Lomholt M, Nielsen SL, Hansen SB, et al. Differential tension between secondary and primary mitral chordae in an acute in-vivo porcine model. *J Heart Valve Dis*. 2002;11:337–345.
22. Clark RE. Stress-strain characteristics of fresh and frozen human aortic and mitral leaflets and chordae tendineae. *J Thorac Cardiovasc Surg*. 1973;66:202–208.
23. Kunzelman KS, Cochran RP. Mechanical properties of basal and marginal mitral valve chordae tendineae. *ASAIO Trans*. 1990;36: M405-M408.
24. Walmsley R. Anatomy of human mitral valve in adult cadaver and comparative anatomy of the valve. *Br Heart J*. 1978;40:351–366.
25. Miller DC. Second order anterior mitral leaflets play a role in preventing systolic anterior motion. *Ann Thorac Surg*. 2002;73:1689–1690.

Influence of Anterior Mitral Leaflet Second-Order Chordae Tendineae on Left Ventricular Systolic Function

Sten Lyager Nielsen, Tomasz A. Timek, G. Randall Green, Paul Dagum, George T. Daughters, J. Michael Hasenkam, Ann F. Bolger, Neil B. Ingels and D. Craig Miller

Circulation. 2003;108:486-491; originally published online July 14, 2003;
doi: 10.1161/01.CIR.0000080504.70265.05
Circulation is published by the American Heart Association, 7272 Greenville Avenue, Dallas, TX 75231

Print ISSN: 0009-7322. Online ISSN: 1524-4539